Protonation in Heteronuclear Diatomic Molecules: Same Molecule, Different Proton Affinities

Emmanuel E. Etim[*] **Oko Emmanuel, Godwin and Sulaiman Adeoye Olagboye**

Abstract. Every heteronuclear diatomic molecular species has two possible sites for protonation giving rise to two possible proton affinity values for a single molecule but experimentally only one proton affinity value is measured for each molecular species with no information regarding where the proton is attached in the molecule. This present work aimed at calculating the proton affinity (PA) of heteronuclear diatomic molecules, specifying which site favors protonation and observing common and rare trends in proton Affinity. In this work, quantum chemical calculations were employed to calculate PA of nitrogen (I) oxide, oxygen monofluoride, carbon(ii)oxie, phosphorus monoxide, silicon(II)oxide, silicon monosulfide, phosphorus mononitride, carbon monosulphide, and phosphorus monosulfide. The indicated that in the heteronuclear diatomic molecules, the best site of protonation corresponds to the most stable protonated analogue, the experimentally assigned value also corresponds to the most stable protonated analogue. These results also aid in indicating the possible factors which could influence the best site of protonation such as bonding nature, stability of the protonated analogue, electron density/electronegativity and Periodic trend.

Key Words: *Protonation; Heteronuclear; Diatomic; Proton affinity PA; Computational methods.*

*Emmanuel E. Etim
Department of Chemical Sciences,
Federal University Wukari, PMB 1020, Wukari,
Taraba State, Nigeria
Email:emmaetim@gmail.com
Orcid id: 0000-0001-8304-9771

Oko Emmanuel, Godwin
Department of Chemical Sciences,
Federal University Wukari, PMB 1020, Wukari,
Taraba State, Nigeria
Email: godwinoko467@gmail.com
Orcid id: 0000-0002-0402-1509

Sulaiman Adeoye Olagboye
Department of Chemistry, Ekiti State University,
Ado -Ekiti, Nigeria

Email: olagboyesa2009@yahoo.com
Orcid id: 0000-0003-4028-2631

I.0   Introduction

A diatomic molecule is a molecule composed of two atoms only, For example, H_2, PO, O_2, CO, NO, N_2, Cl_2, OF, SiO etc Diatomic molecules are either homonuclear i.e they are composed of similar element e.g. H_2, O_2, Cl_2, N_2 or heteronuclear i.e. they are composed of different elements e.g HCl, PO,NO,OF, SiO, H_2O, CO (Emsley, 1989). Homonuclear diatomic molecules typically share equal electrons between the two similar atoms as such have equal electronegativity and are mostly covalently boded where as heteronuclear diatomic molecules even though shares electrons between the two different atoms based on their different quest for stability differ in electronegativity and are mainly covalent with a polar nature which give rise to a dipole (Whitten *et al*., 2010), (Riccardo, 1971), (Taoyi and Thomas 2019), (Casstro *et al*., 1991),(Pauling 1939) and hence, exhibition of infrared absorption band.

Heteronuclear diatomic molecules especially the once containing transition metals have been found to be present in a low-lying electronic state in astronomical bodies. (Tennyson and Yurchenko, 2012), the presence of these molecules in astronomical bodies account for important application of the diatomic molecules in astronomical explorations (Etim *et al*., 2020a). Some applications of these species have been reported in the measurement of magnetic fields in cool stars and brown dwarfs (Johns-Krull *et al*., 1999), in fusion plasmas by (Brezinssek *et al*., 2014; Duxburry, 1998), in laser induced plasmas and discharges, (Chan *et al*., 2013; Vallon *et al*., 2009), in monitoring products of chemical deposition in vapour (Nozaki *et al*., 2000) and atmospheric studies reported by Johnson (1965), (Gole and Kolb, 1981), (Knecht *et al*., 1996). The energy structure of diatomic molecule is also a phenomenon of interest, Coker (2015) and also applied in the study of molecular vibrations, (Vvedensky, 2017) can best be understood via diatomic molecules as starting points.

In protonating a molecule, a proton is added to such a molecule which brings about a change in mass and charge accompanied by a corresponding released of energy called proton affinity (Zumdahl, 1986), (Adam et al., 2010), (Longuet-Higgins, 1956). Certain problems or challenges have been observed in diatomic molecules and from these observations, some diatomic molecules especially heteronuclear diatomic molecules exhibit different proton affinities for the same molecule, the protonation in these group of molecules are also observed to follow a unique trend worthy of redefining proton affinity and also, the molecules show some particular sites in which when protonation occurs appears best with more accurate proton affinity value. These aforementioned problems incited the present research and thus this contribution aims in resolving these problems via the scope of quantum chemical calculations of proton affinity.

2.0 Materials and Methods

Gaussian 09 computational chemistry programs suit was used in calculating the proton affinity (PA), The PA was calculated as the difference in energy (Electronic Energy) between a neutral specie and its protonated analogue (Frisch et al., 2009). Six (6) Ab-initio computational methods were employed for the calculation including Gaussian 04 (G4) compound method, Hartree-Fock (HF) method, Becke, three-parameter, Lee-Yang-Parr (B3LYP) method, Coupled Cluster Single Double CCSD/6-311++G**, Moller-Plesset perturbation theory (MP2) at 6-311++G** and cc-pVDZ basis set. and Moller-Plesset perturbation theory (MP2) at cc-pVDZ basis set were used in carrying out the calculations

These methods were chosen based on the higher degree of accuracy observed in related studies by (Etim *et al*., 2020a), (Etim *et al*., 2018), (Etim *et al*., 2020b), (Etim *et al*.,2016), (Etim *et al*., 2017), (Etim *et al*., 2020c) in which these methods were applied and accurate results were obtained. Also, the use of these methods is essential in monitoring how consistent or coherent the results are.

3.0 Results and Discussion

The results obtained for the protonation study are presented and discussed below in separate headings.

3.1 Nitrogen (I) oxide

Values of PA calculated from calculations different levels of theory are presented in Tables 1a and 1b respectively. The results indicate that the proton energy associated to N atom is closer to the experimentally obtained value of 127.10 kcal/mol as recorded by the NIST chemical web book than on 'O' atom. Also, just as Stability can be deduced from energy values because every system prefer the minimum energy to be stable, this site is the most stable site as seen in table 1(b) containing the Sum of electronic and zero-point Energies, the Optimized geometries of NO and its protonated species are shown in Figs. 1a to 1c in NO, the most stable protonated analogue is protonation along the N site which shows more stability, the stability via this site can be attributed to the bonding nature in the neutral species; oxygen is divalent and it is doubly bonded to nitrogen, thus the oxygen atom has attained stability but the nitrogen atom is trivalent and it is doubly bonded to the divalent oxygen atom. Thus, the nitrogen atom is less stable than the oxygen atom which makes the nitrogen atom more susceptible to protonation. Nature of bonding and Stability of the protonated analogue therefore affects the best site of protonation

Table 1(*a*): Proton Affinity values for NO

Method	Proton attached to N atom		Proton attached to O atom	
	PA (kcal/mol)	Error	PA (kcal/mol)	Error
HF/6-311++G**	101.18	25.92	92.27	34.83
B3LYP/6-311++G**	104.77	22.33	88.59	38.50
MP2/6-311++G**	111.02	16.08	87.52	39.57
MP2/cc-pVDZ	113.59	13.51	89.86	37.24
CCSD/6-311++G**	109.20	17.90	91.19	35.90
G4	109.26	17.84	92.66	34.44
Expt	127.10	NA	127.10	NA

Fig. 1(*a*):Optimized geometry of NO

Fig. 1(*b*):Geometry for protonation at N

Fig. 1(c): Geometry for protonation at O

Table 1(b): Sum of electronic and zero-point Energies for ONH$^+$ and NOH$^+$ molecular species

Method	Energy (Hartree/Particle)*	
	ONH$^+$	NOH$^+$
HF/6-311++G**	-129.442285	-129.428086
B3LYP/6-311++G**	-130.094100	-130.068323
MP2/6-311++G**	-129.773096	-129.756520
MP2/cc-pVDZ	-129.728508	-129.712293
CCSD/6-311++G**	-129.797968	-129.769855
G4	-130.066689	-130.040228

3.2   OF

The results obtained for PA of OF from different functionals are presented in Tables 2a and 2b. From the results, it is evident that the proton affinity of OF to oxygen atom ranged from 58.35 to 62.21 kCal/mol while its affinity to the fluorine atom ranged from 65.66 to 79.18 kcal/mol indicating that for all the functionals, PA for fluorine atom are higher because fluorine is more electronegative than oxygen. These values are however, lower than the experimental values of 121.6 with reference to both oxygen and fluorine.

The large difference between our calculated PA value and the experimental value is a subject of further research to validate the accuracy of the experimental result.

Table 2(a): Proton Affinity values for OF

Method	Proton attached to O atom		Proton attached to F atom	
	PA (kcal/mol)	Error	PA (kcal/mol)	Error
HF/6-311++G**	58.35	63.26	79.18	42.42
B3LYP/6-311++G**	60.41	61.19	65.66	55.94
MP2/6-311++G**	55.95	65.65	66.18	55.42
MP2/cc-pVDZ	58.14	63.46	69.07	52.53
CCSD//6-311++G**	62.21	59.39	70.65	50.95
G4	68.30	53.30	70.92	50.68
Expt	121.6	NA	121.6	NA

The least error observed for the PA value of OF in all the methods here is 42.42 kcal/mol. This value is higher than the least error observed in all of the diatomic species considered in this study. The optimized geometries of OF are presented in Figs. 2a to 2c.

Fig. 2(c) : Geometry for protonation at F

Table 2b: Sum of electronic and zero-point Energies for FOH$^+$ and OFH$^+$ molecular species

Fig. 2(a) : Optimized geometry for OF

Fig. 2(b): Geometry for protonation at O

Method	Energy (Hartree/Particle)*	
	FOH$^+$	OFH$^+$
HF/6-311++G**	-174.266729	-174.299954
B3LYP/6-311++G**	-175.025527	-175.033893
MP2/6-311++G**	-174.631056	-174.647355
MP2/cc-pVDZ	-174.561468	-174.578912
CCSD/6-311++G**	-174.586906	-174.600360
G4	-174.986688	-174.990859

* Sum of electronic and zero-point Energies

3.3   Carbon (II) oxide CO

The protonation in CO follows the most stable protonated analogue i.e the best site of protonation at 'C' which is the site whose PA value is closer to the experimental value, it is also the most stable site. It also follows the bonding nature i.e the factor which influences the stability at that site. The divalency of oxygen is obeyed in the molecule as it is doubly bonded to the carbon atom but the tetravalency of carbon is not obeyed as it is only doubly bonded. Therefore, it is more prone to proton attachment than the oxygen atom which is stabilized by the double bond. Consequently, the proton affinity of the proton attached to carbon is closer to experimental value that that the one attached to oxygen (Table 3a). Deviation between experimental and theoretical values gave error values ranging from -0.93034 to 5.79656 for proton attached to carbon but 34.03449 to 44.36517 for the one attached to oxygen atom (Table 3a). Site is the most stable as seen from the energy values in table 3(b). The geometries are depicted in Figs. 3a to 3c.

Table 3(a): Proton Affinity values for CO

Method	Proton attached to O atom		Proton attached to C atom	
	PA (kcal/mol)	Error	PA (kcal/mol)	Error
HF/6-311++G**	106.1652	35.83481	136.2034	5.79656
B3LYP/6-311++G**	101.9784	40.02155	140.1423	1.857683
MP2/6-311++G**	97.63483	44.36517	144.6089	-2.60893
MP2/cc-pVDZ	98.9984	43.0016	144.6842	-2.68423
CCSD//6-311++G**	104.9516	37.04841	142.6536	-0.65361
G4	107.9655	34.03449	142.9303	-0.93034
Expt	142.0	NA	142.0	NA
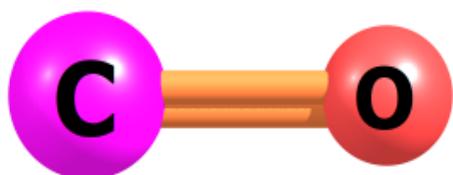
Fig. 3(a):Optimized geometry for CO
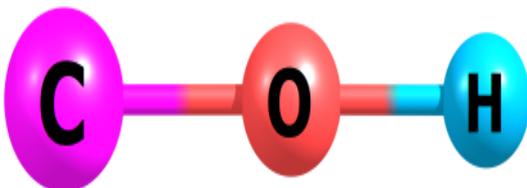
Fig. 3(b): Geometry for protonation at O

Fig.3(c): Geometry for protonation at C

Table 3(b): Sum of electronic and zero-point Energies for COH⁺ and OCH⁺ molecular species

	Energy (Hartree/Particle)*	
	COH⁺	OCH⁺
HF/6-311++G**	-112.934653	-112.982522
B3LYP/6-311++G**	-113.506525	-113.567343
MP2/6-311++G**	-113.228923	-113.303779
MP2/cc-pVDZ	-113.189757	-113.262560
CCSD/6-311++G**	-113.243262	-113.303174
G4	-113.486397	-113.542117

* Sum of electronic and zero-point Energies

3.4. Phosphorus monoxide PO

As seen in from the calculations presented in tables 4(a) and 4(b), PO follows the most stable protonated analogue which is the species where the proton is attached to the oxygen atom.

Table 4(a): Proton Affinity values for PO

Method	Proton attached to O atom		Proton attached to P atom	
	PA (kcal/mol)	Error	PA (kcal/mol)	Error
HF/6-311++G**	177.7025	14.70252	145.377	-17.623
B3LYP/6-311++G**	167.3794	4.379366	140.8771	-22.1229
MP2/6-311++G**	169.4282	6.428184	140.3983	-22.6017
MP2/cc-pVDZ	168.3564	5.356398	138.5873	-24.4127

CCSD//6-311++G**	175.441	12.44098	147.1867	-15.8133
G4	170.793	7.793017	145.7202	-17.2798
Expt	163.0	NA	163.0	NA

It does not follow the bonding pattern as observed in a similar diatomic species (both N and P are in the same group).it is obvious that electron density/electronegativity of oxygen plays a major role in determining the best site of protonation. Their geometries are as contained in Figs. 4a to 4c respectively.

Fig. 4(a) : Optimized geometry for OP
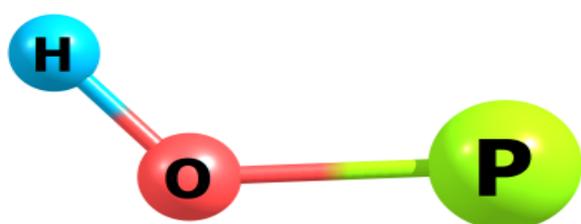
Fig. 4(b) : Geometry for protonation at O
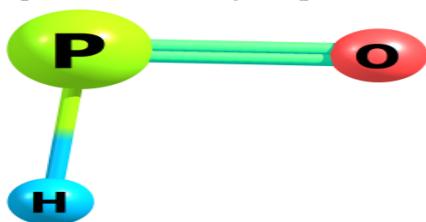
Fig. 4(c): Geometry for protonation at P

Table 3(a): Proton Affinity values for SiO

Table 4(b): Sum of electronic and zero-point Energies for POH$^+$ and OPH$^+$ molecular species

Method	Energy (Hartree/Particle)*	
	POH$^+$	OPH$^+$
HF/6-311++G**	-415.873190	-415.821676
B3LYP/6-311++G**	-416.849071	-416.806837
MP2/6-311++G**	-416.155888	-416.109626
MP2/cc-pVDZ	-416.117194	-416.069754
CCSD/6-311++G**	-416.135894	-416.090868
G4	-416.815808	-416.775852

* Sum of electronic and zero-point Energies

3.5. Silicon (II) oxide

SiO follows the most stable protonated analogue where the proton is attached to the oxygen atom but does not follow the bonding nature as in the case of CO. Both silicon and carbon are in the same group in the periodic table, but exhibit slightly different protonation capacity. Contribution of electron density/electronegativity seems to outweigh bonding nature and play a part in this case too. Tables 5(a) and 5(b) contain the results obtained from the quantum chemical calculations and also from calculations of electronic and zero-point. The geometries are shown in Figs. 5a to 5c

Method	Proton attached to Si atom		Proton attached to O atom	
	PA (kcal/mol)	Error	PA (kcal/mol)	Error
HF/6-311++G**	124.3178	-61.5822	203.0809	17.1809
B3LYP/6-311++G**	125.9593	-59.9407	192.2168	6.3168
MP2/6-311++G**	130.2082	-55.6918	188.3501	2.4501
MP2/cc-pVDZ	132.7534	-53.1466	187.8895	1.9895
CCSD//6-311++G**	130.4304	-55.4696	195.7792	9.8792
G4	129.9139	-55.9861	193.9287	8.0287
Expt	185.9	NA	185.9	NA
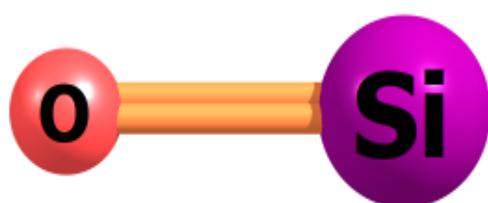
Fig. 5(a): Optimized geometry for SiO

Fig. 5(b): Geometry for protonation at O

Fig. 5(c): Geometry for protonation at Si

Table 5b: Sum of electronic and zero-point Energies for SiOH+ and OSiH+ molecular species

Method	Energy (Hartree/Particle)*	
	SiOH+	OSiH+
HF/6-311++G**	-364.141940	-364.016423
B3LYP/6-311++G**	-365.075092	-364.969504
MP2/6-311++G**	-364.407465	-364.313818
MP2/cc-pVDZ	-364.362311	-364.274446
CCSD/6-311++G**	-364.378997	-364.273789
G4	-365.038645	-364.936631

* Sum of electronic and zero-point Energies

3.6 Silicon monosulfide

In SiS, protonation follows the same patterns as CO in the sense that the experimentally measured PA (in Table 6(a)) value is closer to the protonated analogue in which the proton is attached to silicon atom as in the case of CO where the proton is attached to C atom. However, the protonated analogue in which proton is attached to silicon atom is not the most stable protonated species (as depicted in table 6b) unlike the previous cases above.

Remember that Stability can be deduced from energy values because every system prefers the minimum energy to be stable, sites with lesser energy are more stable. Thus, this species only follows the bonding nature as observed for other diatomic species in this study.

Table 6(a): Proton Affinity values for SiS

Method	Proton attached to Si atom		Proton attached to S atom	
	PA (kcal/mol)	Error	PA (kcal/mol)	Error
HF/6-311++G**	150.2597	0.359652	169.5298	19.62984
B3LYP/6-311++G**	151.3722	1.472227	166.3314	16.43142
MP2/6-311++G**	156.5969	6.696871	166.3835	16.48351
MP2/cc-pVDZ	153.1349	3.234901	164.5273	14.62734
CCSD//6-311++G**	153.7379	3.837937	170.2822	20.38222
G4	154.0605	4.160477	168.9036	19.00359
Expt	149.9	NA	149.9	NA

The optimized geometries of the molecules and its protonated analogues are shown in Figs. 6a to 6c respectively.

Fig. 6(a): Optimized geometry for SSi
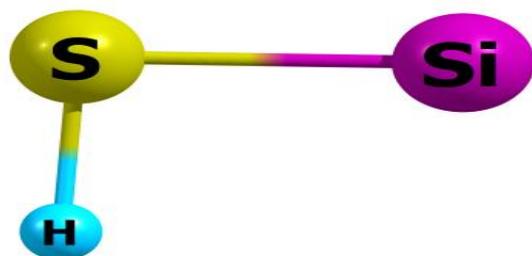
Fig. 6(b): Geometry for protonation at S

Fig. 6(c):Geometry for protonation at Si

Table 6(b): Sum of electronic and zero-point Energies for SSiH+ and SiSH+ molecular species

Method	Energy (Hartree/Particle)*	
	SSiH+	SiSH+
HF/6-311++G**	-686.721131	-686.751840
B3LYP/6-311++G**	-687.984739	-688.008578
MP2/6-311++G**	-686.932544	-686.948140
MP2/cc-pVDZ	-686.927217	-686.945372
CCSD/6-311++G**	-686.949812	-686.976177
G4	-687.946705	-687.970359

* Sum of electronic and zero-point Energies

3.7 Phosphorus mononitride

The experimentally measured PA value for *Phosphorus mononitride* PN are closer to the protonated analogue in which the proton is attached to the N atom. This is found to be the most stable protonated species. Electron density is higher in N atom than in P atom. This may be responsible for the observed trend. These observations are presented in table 7(a)-7(b) and their optimized geometries in Figs. 7a to 7c.

Table 7(a): Proton Affinity values for PN

Method	Proton attached to N atom		Proton attached to P atom	
	PA (kcal/mol)	Error	PA (kcal/mol)	Error
HF/6-311++G**	196.6288	17.42884	90.21766	-88.9823
B3LYP/6-311++G**	190.2722	11.07217	100.4743	-78.7257
MP2/6-311++G**	186.2825	7.082461	107.365	-71.835
MP2/cc-Pvdz	184.2776	5.077568	109.5381	-69.6619
CCSD//6-311++G**	191.4061	12.20608	106.9126	-72.2874
G4	192.9943	13.7943	103.7562	-75.4438
Expt	188.7	NA	188.7	NA

Fig. 7(a): Optimized geometry for NP

Fig. 7(b): Geometry for protonation at N

Fig. 7(c) :Geometry for protonation at P

Table 7(b): Sum of electronic and zero-point Energies for NPH⁺ and PNH⁺ molecular species

Method	Energy (Hartree/Particle)*	
	NPH⁺	PNH⁺
HF/6-311++G**	-395.301469	-395.471046
B3LYP/6-311++G**	-396.262888	-396.404445
MP2/6-311++G**	-395.632181	-395.756471
MP2/cc-pVDZ	-395.609075	-395.728180
CCSD/6-311++G**	-395.603770	-395.738419
G4	-396.231365	-396.373567

* Sum of electronic and zero-point energies

3. 8. Carbon monosulphide CS

CS follows the same trend as CO, the similarity in the trend is due to the fact that both Oxygen and sulfur all belongs to the same group in the periodic table and display some periodic similarity, and as such, some similarities are expected to exist among them because of the effect of periodic trend. The experimentally measured PA value is shown in Table 8(a) to be closer to the protonated species in which the proton is attached to the carbon atom as observed in the case of CO. This protonated analogue is also shown in table 8(b) to be the most stable protonated species. Electron density? Bonding nature? Sulphur is divalent while Carbon is tetravalent, the double bond between C and S, stabilizes the S-atom while C-atom is still left with two unbounded sites thus making it more susceptible for the attachment of a proton (C atom is less stable as compared to the S atom with respect to this CS molecular species). Having shown that proton attached to C atom is more stable from table 8b, this means bonding nature is eminent in this case. Their optimized geometries are contained in Figs. 8a to 8c

Fig. 8(a): Optimized geometry for CS

Table 8(a): Proton Affinity values for CS

Method	Proton attached to C atom		Proton attached to S atom	
	PA (kcal/mol)	Error	PA (kcal/mol)	Error
HF/6-311++G**	184.6221	-2.2138	119.2839	-69.9161
B3LYP/6-311++G**	186.8359	-2.3641	115.3532	-73.8468
MP2/6-311++G**	193.5992	4.3992	113.7323	-75.4677
MP2/cc-pVDZ	191.0948	1.8948	112.771	-76.429
CCSD/6-311++G**	192.1767	2.9767	121.0729	-68.1271
G4	190.409	1.209	119.191	-70.009
Expt	189.2	NA	189.2	NA

Fig. 8(b):Geometry for protonation at C
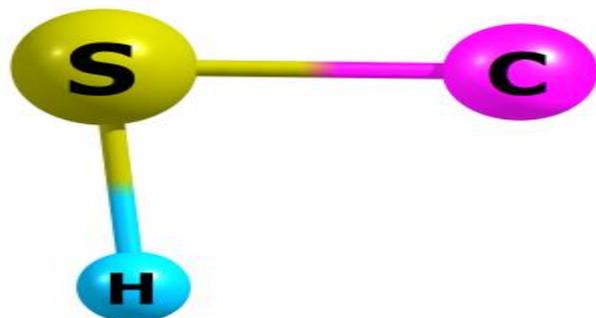
Fig. 8(c): Geometry for protonation at S

Table 8(b): Sum of electronic and zero-point Energies for SCH⁺ and CSH⁺ molecular species

Method	Energy (Hartree/Particle)*	
	SCH⁺	CSH⁺
HF/6-311++G**	-435.629292	-435.525169
B3LYP/6-311++G**	-436.544153	-436.430238
MP2/6-311++G**	-435.895265	-435.767989
MP2/cc-pVDZ	-435.875196	-435.750379
CCSD/6-311++G**	-435.909119	-435.795808
G4	-436.517343	-436.403850

* Sum of electronic and zero-point Energies

3.9. Phosphorus monosulfide

It is evident from the results presented in Table 9a that the protonated analogue for the proton attached to sulphur displayed least error than that of the one attached to phosphorus for all the functionals employed for the calculations (Table 9a).

Table 9(a): Proton Affinity values for PS

Method	Proton attached to P atom		Proton attached to S atom	
	PA (kcal/mol)	Error	PA (kcal/mol)	Error
HF/6-311++G**	165.1875	-1.6125	169.1941	2.3941
B3LYP/6-311++G**	163.2911	-3.5089	165.9122	-0.8878
MP2/6-311++G**	161.0309	-5.7691	166.9652	0.1652
MP2/cc-pVDZ	157.1968	-9.6032	163.6319	-3.1681
CCSD/6-311++G**	167.6191	-0.8191	171.6326	4.8326
G4	165.4498	-1.3502	168.1782	1.3782
Expt	166.8	NA	166.8	NA

This protonated analogue is also found to be more stable. (Table 9b) as compared to the species were the proton is attached to the phosphorus atom. their optimized geometries are presented in figure 9(a) to 9(c)

Fig. 9(a): Optimized geometry for PS

Fig. 9(b): Geometry for protonation at P

Fig. 9(c): Geometry for protonation at S

Table 9(b): Sum of electronic and zero-point Energies for SPH⁺ and CSH⁺ molecular species

Method	Energy (Hartree/Particle)*	
	SPH⁺	CSH⁺
HF/6-311++G**	-738.525136	-738.531521
B3LYP/6-311++G**	-739.827040	-739.831217
MP2/6-311++G**	-738.731176	-738.740633
MP2/cc-pVDZ	-738.729274	-738.739529
CCSD/6-311++G**	-738.770984	-738.777380
G4	-739.789565	-739.793913

* Sum of electronic and zero-point Energies

4.0 Conclusion

Protonation in several heteronuclear diatomic molecular species have been investigated in this study using different basis sets and functionals. The molecules include ***Nitrogen (I) oxide NO, oxygen monofluoride OF, Carbon(ii)oxide CO, Phosphorus monoxide PO, Silicon(ii)oxide SiO, Silicon monosulfide SiS, Phosphorus mononitride PN, Carbon monosulphide CS, and Phosphorus monosulfide PS.*** The results obtained from the calculations were compared to experimental values and it was found out that the calculated proton Affinities of all the diatomic heteronuclear molecules were closer to the experimental values except for NO and OF whose calculated PA seems far apart from the experimental value. For some, protonation follows the most stable protonated analogue (CO, *OF, PO, NO, PN, CS, PS, SiO*) while in SiS, protonation does not follow the most stable protonated analogue. From the forgoing discussions, bonding nature, stability of the protonated analogue, electron density/electronegativity and periodic trend have been identified as factors that could influence the best site proton attachment in heteronuclear diatomic molecules.

5.0 References

Emsley, J. (1989). The Elements. Oxford: Clarendon Press, UK. pp. 22–23.

Whitten, K. W.; Davis, R. E.; Peck, M. L; Stanley, G. G. (2010). *Chemistry* (9th ed.). Brooks/Cole, Cengage Learning. pp. 337–338.

Riccardo, F., (1971) Bonding properties of diatomic molecular orbitals. *Journal of Physical Chemistry*, 75, 19, pp. 3012-3014. DOI: 10.1021/J100688a024

Taoyi, C., & Thomas, A. M. (2019). Bond orders of the diatomic molecules. *RSC Advances*, 9, pp. 17072-17092.

Castro, M., Keller, J., & Mareca, P., (1991). Bonding in heteronuclear transition metal diatomics: Nblr. *International Journal of Quantum Chemistry*, 39, 5, pp 649-754.

Pauling, L. (1939). *Nature of the chemical bond.* Cornell University press, Ithaca, 1939, p.70

Tennnyson J. &Yurchenko S. N. (2012). ExoMol:molecular Line Lists for exoplanet and otheratmospheres. Mon. Not. R. Astron. Soc. 425, 1, pp. 21-33.

Etim E. E., Chrisanthus A., Usman L., Ifeoma Sandra U. & Etiowo George Ukpong, (2020a) Protonation of carbonyl sulphide: Ab-initio. *Journal of Applied Sciences*, 20, pp. 26-34

Johns-Krull C. M., Valenti J. A. & Koresko C., (1999), Measuring the Magnetic Fieldon the Classical T Tauri Star BP *Tauri Astrophysics Journal*, 516, pp. 900-915.

Brezinsek, S., Stamp, M. F., Nishijima, D., Borodin, D., Devaux, S., Krieger, K., Marsen, S., O'Mullane, M., Bjoerkas, C/. & Kirschner A. (2014). *Study of physical and chemical assisted physical sputtering of beryllium in the JET ITER-like wall.* Proceeding of IAEA Technical Meeting on energetic particles in magnetic confinement systems, Peking, China.

Vallon R.; Ashworth S.H.; Crozet P.; Field R.W.; Forthomme D.; Harker H.; Richard C.; & Ross A.J.;(2009). Room-temperature metal-hydride discharge source, with observations on NiH and FeH. *Journal of Physical Chemistry*,. A 113, pp.13159-13166.

Chan M. C., Yeung S. H., Wang N. & Cheung A. S. C. (2013). Laser absorption spectroscopy of the $d^3\Pi_g \leftarrow c^3\Sigma_u^+$ transition of C_2. *Journal of Physical Chemistry*, A 117, pp. 9578-9583.

Nozaki, Y., Kongo K., Miyazaki, T., Kitazoe M., Horii, K., Umemoto, H., Masuda, A. & Matsumura, H. (2000). Identification of Si and SiH in catalytic chemical vapor deposition of SiH_4SiH_4 by laser induced fluorescence spectroscopy. *Journal of Applied Physics*, 88, pp. 5437-5443.

Johnson E.R.;(1965). Twilight resonance radiation of AlO in the upper atmosphere. *Journal of Geophysical Research*, 70, pp. 1275-1277.

Gole J. L. & Kolb C. E. (1981). On the upper atmospheric chemiluminescent emission observed upon release of aluminum vapor and its compounds. *Journal of Geophysical Research: Space Physics*, 86, pp.9125-9136.

Knecht D.J.; Pike C.P.; Murad E.; Rall D.L.A.; (1996). Interaction of solid-rocket exhaust with the atmosphere. *Journal of Spacecraft and Rockets*, 33, pp. 677-685.

Coker, J. (2015) *Applications of diatomic molecules*; Ph.D Dissertation, University of Oklahoma Graduate College.

Vvedensky D. D. (2017) *Encyclopedia of spectroscopy and spectrometry* (Third Edition), Elsevier, 978-0-12-803224-4. https://doi.org/10.1016/B978-04442227-6/50005-3

Zumdahl, S. S. (1986) *Chemistry*. Lexington, MA: Heath. ISBN 0-669-04529-2.

Adam M., Kevin R., Darrin M. Y (2010). Accurate proton affinity and gas-phased basicity values for molecules important in biocatalysis. *Journal of Physical Chemistry* B.114, 43, pp. 13911-13921

Longuet-Higgins H.C.,(1956) Proton affinities, recueil des Travaux Chimiques des Pays-B, Volume 75, issue 7.https://doi.org/10.1002/recl.19560750718

Frisch, M.J.; Toucks, G.W.; Schlegel, H.B.; Scuseria G.E.; Robb, M.A.; Cheeseman, J.R.; Scalmani, G.; Baron, V.; Mennucci, B.; Peterson, G.A., (2009) *Gaussian 09 revision* D.01; Gaussian, Inc., Wallingford, CT.

Etim, E. E., Oko, G. E., Onen, A. I., Ushie O. A., Andrew, C., Lawal, U. & Khanal, G. P. (2018). Computational Studies of Sulphur trioxide (SO_3) and its protonated analogues. *Journal of Chemical Society of Nigeria*, 43, 2, pp 10-17

Etim, E. E., Chrysanthus, A., Lawal, U., Ifeoma, S. U. & Etiowo, G. U. (2020b). Protonation of Carbonyl Sulfide: Ab-initio study. *Journal of Applied Sciences*, 20, pp. 26-34

Etim, E. E. & Arunan, E.,(2016). Interstellar isomeric species, energy, stability and abundance relationship. *European Physics Journal.Plus,* pp. 131, 12, https://doi.org/10.1140/epje/i2016-1644-8-0

Etim, E. E., Abah, B. S., Mbakara, I. E., Inyang, E. J. & Ukafia, O. P. (2017) Quantum Chemical Calculations on Silicon Monoxide (SiO) and its Protonated Analogues. *Tropical Journal of Applied Natural Sciences*, 2, pp. 61-68..

Etim, E. E., Sulaiman, A. O., Oko, E. G. & Irene M. A., (2020c) Quantum Chemical studies on Silicon tetrafluoride and its protonated analogues. *International Journal of Modern Chemistry, 12, 1,* pp 26-45.

Conflict of Interest
The authors declared no conflict of interest.